LBNL-40820
UC-405
Preprint

ERNEST ORLANDO LAWRENCE BERKELEY NATIONAL LABORATORY

Demosaicing: Image Reconstruction from Color CCD Samples

Ron Kimmel

Computing Sciences Directorate

Mathematics Department

September 1997

To be submitted
for publication

REFERENCE COPY
Does Not
Circulate
Bldg. 50 Library - Ref.
Lawrence Berkeley National Laboratory
Copy 1
LBNL-40820

DISCLAIMER

This document was prepared as an account of work sponsored by the United States Government. While this document is believed to contain correct information, neither the United States Government nor any agency thereof, nor the Regents of the University of California, nor any of their employees, makes any warranty, express or implied, or assumes any legal responsibility for the accuracy, completeness, or usefulness of any information, apparatus, product, or process disclosed, or represents that its use would not infringe privately owned rights. Reference herein to any specific commercial product, process, or service by its trade name, trademark, manufacturer, or otherwise, does not necessarily constitute or imply its endorsement, recommendation, or favoring by the United States Government or any agency thereof, or the Regents of the University of California. The views and opinions of authors expressed herein do not necessarily state or reflect those of the United States Government or any agency thereof or the Regents of the University of California.

LBNL-40820

DEMOSAICING: IMAGE RECONSTRUCTION FROM COLOR CCD SAMPLES*

Ron Kimmel

Lawrence Berkeley National Laboratory
and
Mathematics Department
University of California
Berkeley, CA 94720

September 1997

*This work was supported in part by the Applied Mathematical Sciences subprogram of the Office of Energy Research, U.S. Department of Energy, under Contract DE-AC03-76SF00098, and by the Office of Naval Research under Grant N00014-96-1-0381.

Demosaicing: Image Reconstruction from Color CCD Samples *

Ron Kimmel
Lawrence Berkeley National Laboratory
and Dept. of Mathematics
University of California, Berkeley, CA 94720

Abstract

A simplified color image formation model is used to construct an algorithm for image reconstruction from CCD sensors' samples. The proposed method involves two successive steps. The first is motivated by Cok's [1] template matching technique, while the second step uses steerable inverse diffusion in color. Classical linear signal processing techniques tend to over smooth the image and result in noticeable color art effects along edges and sharp features. The question is how should the different color channels support each other to form the best possible reconstruction. Our answer is to let the edges support the color information, and the color channels support the edges, and thereby achieve better perceptual results than those that are bounded by the sampling theoretical limit.

1 Introduction

In recent years, digital cameras for still images and movies became popular. There are many obvious advantages to digital images comparing to classical film based cameras, yet there are limitations as well. For example, the spatial resolution is limited due to the physical structure of the sensors. 'Super resolution' beyond the sensors resolution can be achieved by considering a sequence of images.

In this note we deal with the reconstruction of a single color digital image from its color CCD sensors' information. We limit our discussion to Bayer color filter array (CFA) pattern as presented in Figure 1. We will start with a simple color image formation model and explore the relation between the different color channels such that the channels support the edges, and the edges support the colors. This relation with a simple color image formation model enables a reconstruction beyond the linear optimal signal processing approach that is limited by the Nyquist sampling rate.

*This work is supported in part by the Applied Mathematics Subprogram of the Office of Energy Research under DE-AC03-76SFOOO98, and ONR grant under NOOO14-96-1-0381.

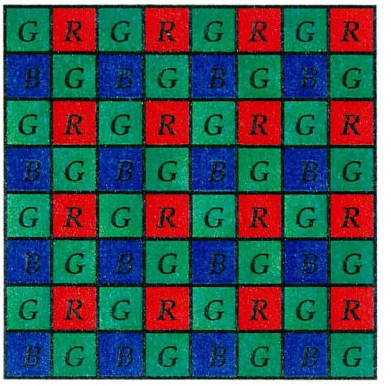

Figure 1: Bayer CFA (color filter array) pattern (US Patent 3,971,065, 1976).

We follow Cok's [1] exposition for constructing the first step of the algorithm: The reconstruction stage. The Green component is reconstructed first with the help of the Red and Blue gradients. Then the Red and Blue are reconstructed using the Green values, edge approximations, and a simple color ratio rule: Within a given 'object' the ratio $Red/Green$ is locally constant (the same is true for $Blue/Green$). This rule falls apart across edges where the color gradients are high, which are the interesting and problematic locations from our reconstruction point of view.

Next the Green, Red, and Blue pixels are adjusted to fit the color cross ratio equivalence. The interpolation and the adjustment are weighted by a function of the directional derivatives to reduce the influence of ratios across edges. This is the main difference from Cok's [1] method, who try to match templates that predict the local structure of the image for a bilinear interpolation.

The second step, the enhancement stage, involves an anisotropic inverse diffusion flow in color space, which is an extension of Weickert's gray level texture enhancement method [12], Gabor's geometric filter [6], and is based on the geometrical framework for color introduced in [11, 8]. It is also related to the recent results of Sapiro and Ringach [10], and Cottet and El Ayyadi [2]. The idea is to consider the color image as a two dimensional surface in 5D (x, y, R, G, B) space, extract its induced metric and smooth the metric in order to sense the structure of the image surface beyond the local noise. Then diffuse the different channels along the edges and simultaneously enhance the image by applying an 'inverse heat' operator across the edges.

The structure of this note is as follows: Section 2 introduces a simple model for color images. Next, Section 3 uses this model for the reconstruction of a 1D image. Section 4 presents the first step of the algorithm, the reconstruction stage, that involves weighted interpolation subject to constant cross ratio of the spectral channels. Section 5 presents the second step of the algorithm. It is a non linear enhancement filter based on steerable anisotropic inverese diffusion flow in color space. Section 5 concludes with experimental results on a set of benchmark images.

2 A Simple Color Image Formation Model

A simplified model for color images is a result of viewing Lambertian non flat surface patches. Such a scene is a generalization of what is known as a 'Mondriaan world'. According to the model, each channel may be considered as the projection of the real 3D world surface normal $\hat{\mathbf{N}}(\mathbf{x})$ onto the light source direction $\vec{l}$, multiplied by the albedo $\rho(x, y)$. The albedo captures the characteristics of the 3D object's material, and is different for each of the spectral channels. That is, the 3 color channels may be written as

$$\begin{aligned} I^R(\mathbf{x}) &= \rho_R(\mathbf{x})\hat{\mathbf{N}}(\mathbf{x}) \cdot \vec{l} \\ I^G(\mathbf{x}) &= \rho_G(\mathbf{x})\hat{\mathbf{N}}(\mathbf{x}) \cdot \vec{l} \\ I^B(\mathbf{x}) &= \rho_B(\mathbf{x})\hat{\mathbf{N}}(\mathbf{x}) \cdot \vec{l}. \end{aligned} \tag{1}$$

This means that the different colors capture the change in material via ρ_i (where i stands for R, G, B) that multiplies the normalized shading image $\tilde{I}(\mathbf{x}) = \hat{\mathbf{N}}(\mathbf{x}) \cdot \vec{l}$. The Mondriaan color image formation model [4] was used for color based segmentation [7] and shading extraction from color images [5]. Let us follow the above generalization of this model and assume that the material, and therefore the albedo, are the same within a given object in the image, e.g. $\rho_i(\mathbf{x}) = c_i$, where c_i is a given constant. Thus, within the interior of a given object the following constant ratio holds:

$$\frac{I^i(\mathbf{x})}{I^j(\mathbf{x})} = \frac{\rho_i(\mathbf{x})\tilde{I}(\mathbf{x})}{\rho_j(\mathbf{x})\tilde{I}(\mathbf{x})} = \frac{\rho_i(\mathbf{x})}{\rho_j(\mathbf{x})} = \frac{c_i}{c_j} = \text{constant}. \tag{2}$$

That is, the color ratio within a given object is constant. We note, that this is an oversimplified assumption for general analysis of color images. However, its local nature makes it valid and useful for our technological purpose.

3 The 1D Case

Let us start with a simple 1D example with two colors, see Fig. 2. Our assumption is that the colors are smooth within a given object and go through a sudden jump at the boundaries. Define the central difference approximation to be $D_x I_i \equiv \frac{I_{i+1} - I_{i-1}}{\Delta x}$, where $I_i \equiv I(i\Delta x)$ is the value of the function $I(x)$ at the point $x = i\Delta x$, and Δx is the spatial discretization interval.

Given the samples (odd points for the Red and even points for the Green) we use the gradient to construct an edge indicator for the interpolation. Let the edge indicator be $e_i^g = f(D_x G_i)$, where $f(\circ)$ is a decreasing function, e.g. $e_i^g = (1 + (D_x G_i)^2)^{-1/2}$, and respectively e_i^r. One simple reconstruction procedure is as follows:

- <u>Init:</u> Interpolate for the Green at the missing points

$$G_i = \frac{e_{i-1}^r G_{i-1} + e_{i+1}^r G_{i+1}}{e_{i-1}^r + e_{i+1}^r}.$$

- <u>Repeat for 3 times:</u>

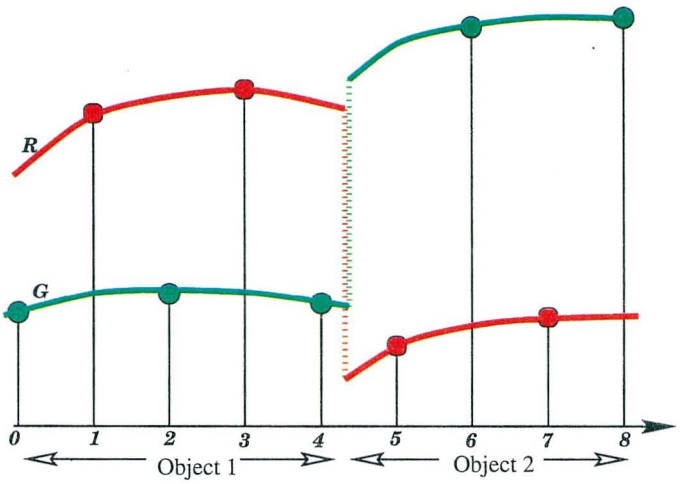

Figure 2: The Red and Green components of a 1D image.

- Interpolate the Red values via the ratio rule weighted by the edge indicator

$$R_i = G_i \frac{e^g_{i-1}\frac{R_{i-1}}{G_{i-1}} + e^g_{i+1}\frac{R_{i+1}}{G_{i+1}}}{e^g_{i-1} + e^g_{i+1}}.$$

- Correct the Green values to fit the ratio rule

$$G_i = R_i \frac{e^r_{i-1}\frac{G_{i-1}}{R_{i-1}} + e^r_{i+1}\frac{G_{i+1}}{R_{i+1}}}{e^r_{i-1} + e^r_{i+1}}.$$

- <u>End of loop</u>.

Note that this is a numerically consistent procedure for the proposed color image formation model. It means that as the sampling grid is refined, the result converges to the continuous solution.

Here, again we recognize the importance of segmentation in computer vision. An accurate segmentation procedure, that gives the exact locations of the objects boundaries, would have allowed an image reconstruction far beyond the sampling limit (under the assumption that within a given object there are no high spatial frequencies).

4 First Step: Reconstruction

For real 2D images with three color channels the reconstruction is less trivial. Edges now become curves rather than points, and in many cases one needs to interpolate missing points along the edges. We would still like to avoid interpolating across edges.

Based on the simplified color image formation model, the three channels go through a sudden jump across the edges. Thus, the gradient magnitude can be used as an edge

indicator, and its direction can approximate the edge direction (it is easy to verify that the gradient ∇G is normal to the level set curves of $G(\mathbf{x})$, i.e. $G(\mathbf{x}) = const.$)

The directional derivatives are approximated at each point based on its 8 nearest neighbors on the grid. Define the finite difference approximation for the directional derivatives, central D, forward D^+, and backwards D^-, as follows:

$$\begin{cases} D_x G_{i,j} = \frac{G_{i+1,j} - G_{i-1,j}}{2\Delta x} & D_y G_{i,j} = \frac{G_{i,j+1} - G_{i,j-1}}{2\Delta y} \\ D_{x'} G_{i,j} = \frac{G_{i+1,j+1} - G_{i-1,j-1}}{2\sqrt{\Delta x^2 + \Delta y^2}} & D_{y'} G_{i,j} = \frac{G_{i-1,j+1} - G_{i+1,j-1}}{2\sqrt{\Delta x^2 + \Delta y^2}} \\ D^+_{x'} G_{i,j} = \frac{G_{i+1,j+1} - G_{i,j}}{\sqrt{\Delta x^2 + \Delta y^2}} & D^-_{x'} G_{i,j} = \frac{G_{i+1,j+1} - G_{i,j}}{\sqrt{\Delta x^2 + \Delta y^2}} \\ D^+_{y'} G_{i,j} = \frac{G_{i-1,j+1} - G_{i,j}}{\sqrt{\Delta x^2 + \Delta y^2}} & D^-_{y'} G_{i,j} = \frac{G_{i,j} - G_{i+1,j-1}}{\sqrt{\Delta x^2 + \Delta y^2}} \end{cases} \tag{3}$$

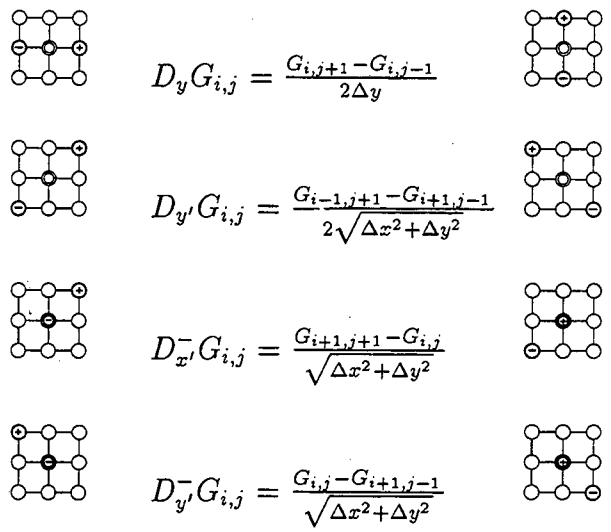

At the Green points use $\max\{|D^+_{x'} G_{i,j}|, |D^-_{x'} G_{i,j}|\}$ for the magnitude of the directional derivative along the x' direction (and similarly for y'). For the rest of the points and the x and y directions use central differences. We thereby construct an approximation for the direction derivatives at each and every point. Denote these approximations as $Dx_{ij}, Dy_{ij}, Dx'_{ij}$, and Dy'_{ij}, respectively.

Next, we generalize an edge indicator function. When a point at location $((i+1)\Delta x, j\Delta y)$ is taking part in the interpolation at the $(i\Delta x, j\Delta y)$ location, we use the following weight as an edge indicator: $e_{ij}^{i+1,j} = (1 + {Dx_{ij}}^2 + {Dx_{i+1,j}}^2)^{-1/2}$

Based on the edge indicators as weights for the interpolation we follow similar steps as for the 1D case to reconstruct the 2D image:

- <u>Init:</u> Interpolate for the Green at the missing points

$$G_{ij} = \frac{e_{ij}^{i-1,j} G_{i-1,j} + e_{ij}^{i+1,j} G_{i+1,j} + e_{ij}^{i,j-1} G_{i,j-1} + e_{ij}^{i,j+1} G_{i,j+1}}{e_{ij}^{i-1,j} + e_{ij}^{i+1,j} + e_{ij}^{i,j-1} + e_{ij}^{i,j+1}}.$$

  Interpolate for the Blue and Red in two steps.
  Step 1 (interpolate missing Blue at Red locations) :

$$B_{ij} = G_{ij} \frac{e_{ij}^{i+1,j+1} \frac{B_{i+1,j+1}}{G_{i+1,j+1}} + e_{ij}^{i-1,j-1} \frac{B_{i-1,j-1}}{G_{i-1,j-1}} + e_{ij}^{i-1,j+1} \frac{B_{i-1,j+1}}{G_{i-1,j+1}} + e_{ij}^{i+1,j-1} \frac{B_{i+1,j-1}}{G_{i+1,j-1}}}{e_{ij}^{i+1,j+1} + e_{ij}^{i-1,j-1} + e_{ij}^{i-1,j+1} + e_{ij}^{i+1,j-1}}.$$

  Step 2 (interpolate at the rest of the missing Blue points):

$$B_{ij} = G_{ij} \frac{e_{ij}^{i+1,j} \frac{B_{i+1,j}}{G_{i+1,j}} + e_{ij}^{i-1,j} \frac{B_{i-1,j}}{G_{i-1,j}} + e_{ij}^{i,j+1} \frac{B_{i,j+1}}{G_{i,j+1}} + e_{ij}^{i,j-1} \frac{B_{i,j-1}}{G_{i,j-1}}}{e_{ij}^{i+1,j} + e_{ij}^{i-1,j} + e_{ij}^{i,j+1} + e_{ij}^{i,j-1}}.$$

Interpolate the Red with two similar steps.

- Repeat for 3 times:
- Correct the Green values to fit the ratio rule

$$\begin{aligned} G_{ij}^{B} &= B_{ij}(e_{ij}^{i+1,j}\frac{G_{i+1,j}}{B_{i+1,j}} + e_{ij}^{i-1,j}\frac{G_{i-1,j}}{B_{i-1,j}} + e_{ij}^{i,j+1}\frac{G_{i,j+1}}{B_{i,j+1}} + e_{ij}^{i,j-1}\frac{G_{i,j-1}}{B_{i,j-1}} \\ &+ e_{ij}^{i+1,j+1}\frac{G_{i+1,j+1}}{B_{i+1,j+1}} + e_{ij}^{i-1,j-1}\frac{G_{i-1,j-1}}{B_{i-1,j-1}} + e_{ij}^{i-1,j+1}\frac{G_{i-1,j+1}}{B_{i-1,j+1}} + e_{ij}^{i+1,j-1}\frac{G_{i+1,j-1}}{B_{i+1,j-1}})/ \\ &(e_{ij}^{i+1,j} + e_{ij}^{i-1,j} + e_{ij}^{i,j+1} + e_{ij}^{i,j-1} + e_{ij}^{i+1,j+1} + e_{ij}^{i-1,j-1} + e_{ij}^{i-1,j+1} + e_{ij}^{i+1,j-1}). \end{aligned} \tag{4}$$

and average between the Blue and Red interpolation results

$$G_{ij} = \frac{G_{ij}^{B} + G_{ij}^{R}}{2}.$$

- Correct the Blue and Red values via the ratio rule weighted by the edge indicator

$$\begin{aligned} B_{ij} &= G_{ij}(e_{ij}^{i+1,j}\frac{B_{i+1,j}}{G_{i+1,j}} + e_{ij}^{i-1,j}\frac{B_{i-1,j}}{G_{i-1,j}} + e_{ij}^{i,j+1}\frac{B_{i,j+1}}{G_{i,j+1}} + e_{ij}^{i,j-1}\frac{B_{i,j-1}}{G_{i,j-1}} \\ &+ e_{ij}^{i+1,j+1}\frac{B_{i+1,j+1}}{G_{i+1,j+1}} + e_{ij}^{i-1,j-1}\frac{B_{i-1,j-1}}{G_{i-1,j-1}} + e_{ij}^{i-1,j+1}\frac{B_{i-1,j+1}}{G_{i-1,j+1}} + e_{ij}^{i+1,j-1}\frac{B_{i+1,j-1}}{G_{i+1,j-1}})/ \\ &(e_{ij}^{i+1,j} + e_{ij}^{i-1,j} + e_{ij}^{i,j+1} + e_{ij}^{i,j-1} + e_{ij}^{i+1,j+1} + e_{ij}^{i-1,j-1} + e_{ij}^{i-1,j+1} + e_{ij}^{i+1,j-1}). \end{aligned} \tag{5}$$

- End of loop.

Up to this point, the original values given as samples were not modified. We have interpolated the missing points weighted by edge indicator functions subject to the constant cross ratio. Next, we apply inverse diffusion in color to the whole image as an enhancement filter.

5 Second Step: Enhancement

This section is a brief description of one of the non linear filters introduced in [8] that we apply as a second step for enhancing the color image.

In [6], Gabor considered an image enhancement procedure based on an anisotropic flow via the inverse second directional derivative in the 'edge' direction and the geometric heat equation as a diffusion along the edge, see also [9]. Cottet and Germain [3] used a smoothed version of the image to direct the diffusion. Weickert [12] smoothed the 'structure tensor' $\nabla I \nabla I^T$ and then manipulated its eigenvalues to steer the smoothing direction, while Sapiro and Ringach [10] eliminated one eigenvalue from the structure tensor in color space without smoothing its coefficients.

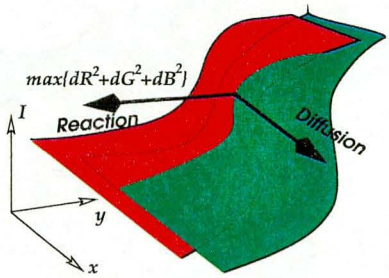

Figure 3: The Red and Green components painted as surfaces in x, y, I with the inverse diffusion (across the edge) and diffusion (along the edge) directions.

Motivated by all of these results, a new color enhancement filter was introduced in [8]. The inverse diffusion and diffusion directions are deduced from the smoothed metric coefficients $g_{\mu\nu}$ of the image surface. The color image is considered as a 2D surface in the 5D (x, y, R, G, B) space, as suggested in [11]. The induced metric coefficients are extracted for the image surface and used as a natural structure tensor for the color case.

The induced metric $(g_{\mu\nu})$ is a symmetric matrix that captures the geometry of the image surface. Let λ_1 and λ_2 be the largest and the smallest eigenvalues of $(g_{\mu\nu})$, respectively. Since $(g_{\mu\nu})$ is a symmetric positive matrix its corresponding eigenvectors u_1 and u_2 can be chosen orthonormal. Let $U \equiv (u_1|u_2)$, and $\Lambda \equiv \begin{pmatrix} \lambda_1 & 0 \\ 0 & \lambda_2 \end{pmatrix}$, then we readily have the equality

$$(g_{\mu\nu}) = U\Lambda U^T. \tag{6}$$

Note also that

$$(g^{\mu\nu}) \equiv (g_{\mu\nu})^{-1} = U\Lambda^{-1}U^T = U \begin{pmatrix} 1/\lambda_1 & 0 \\ 0 & 1/\lambda_2 \end{pmatrix} U^T, \tag{7}$$

and that

$$g \equiv \det(g_{\mu\nu}) = \lambda_1\lambda_2. \tag{8}$$

Let us use the image metric as a structure tensor. We extract the structure from the metric $(g_{\mu\nu})$ and then modify it to be a non-singular symmetric matrix with one positive and one negative eigenvalues. That is, instead of diffusion we introduce a controlled inverse diffusion in the edge direction. This is an extension of Gabor's idea [6] of inverting the diffusion along the gradient direction, see Fig. 3.

The proposed inverse diffusion enhancement for color images is then given as follows:

1. Compute the metric coefficients $g_{\mu\nu}$.

$$g_{\mu\nu} = \delta_{\mu\nu} + \sum_{k=\{R,G,B\}} I^k_\mu I^k_\nu. \tag{9}$$

or explicitly

$$(g_{\mu\nu}) = \begin{pmatrix} 1 + R_x^2 + G_x^2 + B_x^2 & R_x R_y + G_x G_y + B_x B_y \\ R_x R_y + G_x G_y + B_x B_y & 1 + R_y^2 + G_y^2 + B_y^2 \end{pmatrix} \tag{10}$$

2. Diffuse the $g_{\mu\nu}$ coefficients by convolving with a Gaussian of variance ρ, thereby

$$\tilde{g}_{\mu\nu} = G_\rho * g_{\mu\nu}. \tag{11}$$

Where $G_\rho = e^{-(x^2+y^2)/\rho^2}$.

3. Change the eigenvalues of $(\tilde{g}_{\mu\nu})$ such that the largest eigenvalue λ_1 is now $\lambda_1 = -\alpha^{-1}$ and $\lambda_2 = \alpha$, for some given positive scalar $\alpha < 1$. This yields a new <u>matrix</u> $\hat{g}_{\mu\nu}$ that is given by:

$$(\hat{g}_{\mu\nu}) = \tilde{U} \begin{pmatrix} -\alpha^{-1} & 0 \\ 0 & \alpha \end{pmatrix} \tilde{U}^T = \tilde{U} \Lambda_\alpha \tilde{U}^T. \tag{12}$$

4. Evolve the k-th channel via the flow:

$$\begin{aligned} I_t^k &= \partial_\mu \hat{g}^{\mu\nu} \partial_\nu I^k \\ &= \operatorname{div}\left(\tilde{U} \begin{pmatrix} -\alpha & 0 \\ 0 & \alpha^{-1} \end{pmatrix} \tilde{U}^T \nabla I^k \right). \end{aligned} \tag{13}$$

Inverting the heat equation is an inherently unstable process. However, if we keep smoothing the metric coefficients, and apply the diffusion along the edge (given the positive eigenvalue), we get a coherence-enhancing flow that yields sharper edges and is stable for a short duration of time.

6 Experimental Results

We tested the proposed method on four benchmark images that were sampled with Bayer color filter array pattern. See Figure 4. The same parameters are used for the reconstruction in all the examples, i.e. case dependent tuning was not used for the different images. As a reference we present the result of a bilinear interpolation for the missing points for each channel separately.

7 Acknowledgments

I thank Prof. James Sethian for helpful discusions, and to Dr. Yacov Hel-Or for introducing the problem and supplying the color benchmark images.

Figure 4: Reconstruction and enhancement results for four benchmark images: Statue, Sails, Window, and Lighthouse. For each case, top left is the original image, top right is reconstruction by simple bilinear interpolation, bottom left is the first step reconstruction, and bottom right is the second step enhancement result.

References

[1] D R Cok. Reconstruction of CCD images using template matching. In *Proc. of IS&T's Annual Conference/ICPS*, pages 380–385, 1994.

[2] G H Cottet and M El Ayyadi. A Volterra type model for image processing. *IEEE Trans. on IP*, to appear, 1997.

[3] G H Cottet and L Germain. Image processing through reaction combined with nonlinear diffusion. *Math. Comp.*, 61:659–673, 1993.

[4] P T Eliason, L A Soderblom, and P S Chavez. Extraction of topographic and spectral albedo information from multi spectral images. *Photogrommetric Engineering and Remote Sensing*, 48:1571–1579, 1981.

[5] B V Funt, M S Drew, and M Brockington. Recovering shading from color images. In G Sandini, editor, *Lecture Notes in Computer Science, 588, Computer Vision: ECCV'92*, pages 124–132. Springer-Verlag, 1992.

[6] D Gabor. Information theory in electron microscopy. *Laboratory Investigation*, 14(6):801–807, 1965.

[7] G Healey. Using color for geometry-insensitive segmentation. *J. Opt. Soc. Am. A*, 6:920–937, 1989.

[8] R Kimmel, R Malladi, and N Sochen. Images as embedding maps and minimal surfaces: Movies, color, texture, and volumetric medical images. *IEEE Trans. on PAMI*, submitted, 1997.

[9] M Lindenbaum, M Fischer, and A M Bruckstein. On Gabor's contribution to image enhancement. *Pattern Recognition*, 27(1):1–8, 1994.

[10] G Sapiro and D L Ringach. Anisotropic diffusion of multivalued images with applications to color filtering. *IEEE Trans. Image Proc.*, 5:1582–1586, 1996.

[11] N Sochen, R Kimmel, and R Malladi. A general framework for low level vision. *IEEE Trans. on Image Processing*, to appear, 1997.

[12] J Weickert. *Anisotropic diffusion in image processing.* Ph.D. thesis, Kaiserslautern Univ., Kaiserslautern, Germany, November 1995.

Original

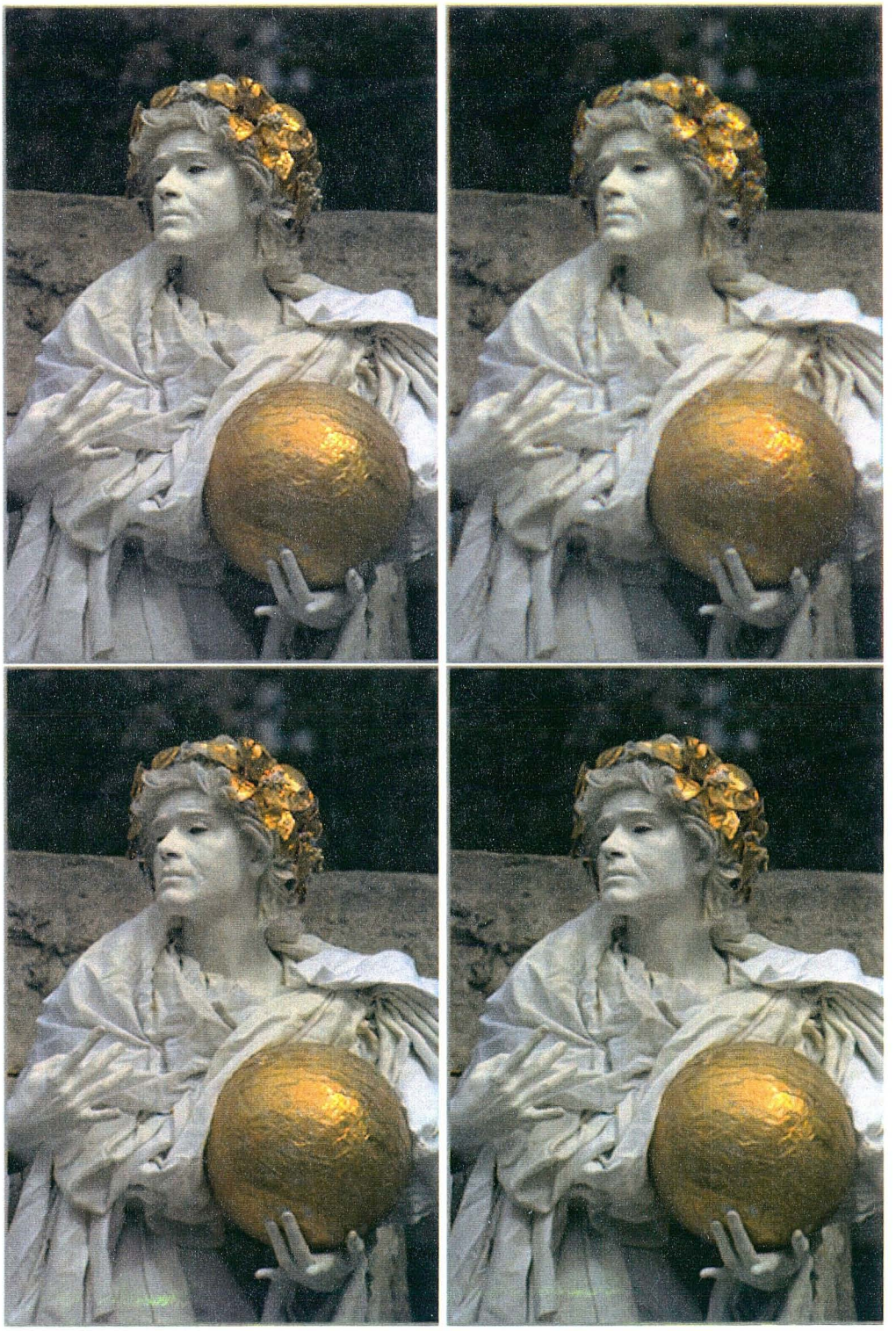

Original

Original

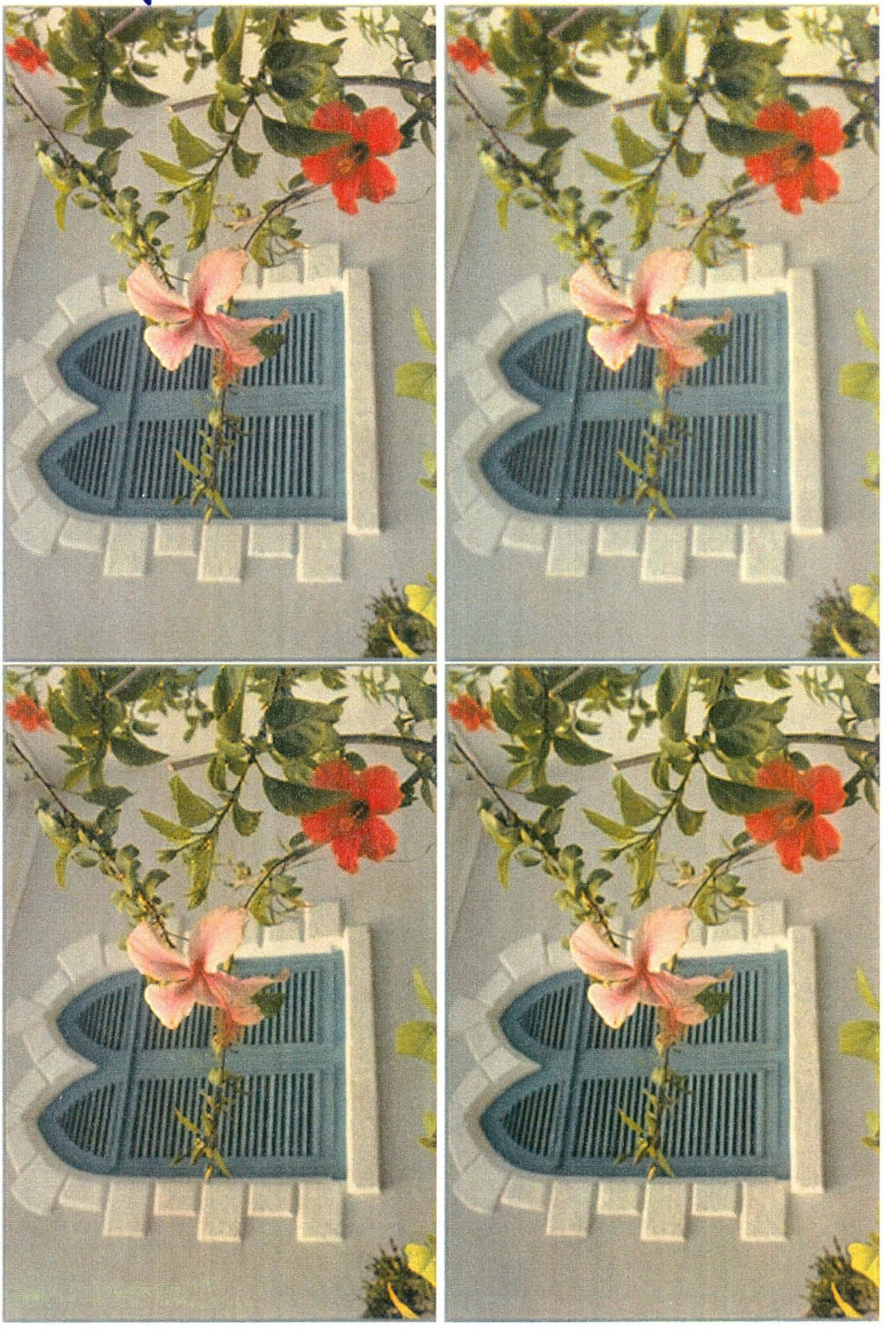

Original

Ernest Orlando Lawrence Berkeley National Laboratory
One Cyclotron Road | Berkeley, California 94720

Prepared for the U.S. Department of Energy under Contract No. DE-AC03-76SF00098